**INTERNATIONAL JOURNAL OF OPTIMIZATION IN CIVIL ENGINEERING**
***Int. J. Optim. Civil Eng., 2011; 3:397-417***

# TOPOLOGY OPTIMIZATION OF COMPOSITE MATERIALS WITH OPTIMAL STIFFNESS AND THERMAL CONDUCTIVITY

X.Y. Yang[1 *, †], X. Huang[1], Y.M. Xie[1], Q. Li[2] and J.H. Rong[3]
[1]*School of Civil, Environmental and Chemical Engineering, RMIT University, GPO Box 2476, Melbourne 3001, Australia*
[2]*School of Aerospace, Mechanical and Mechatronic Engineering, The University of Sydney, NSW 2006, Australia*
[3]*School of Automotive and Mechanical Engineering, Changsha University of Science and Technology, Changsha 410076, China*

## ABSTRACT

This paper presents the bidirectional evolutionary structural optimization (BESO) method for the design of two-phase composite materials with optimal properties of stiffness and thermal conductivity. The composite material is modelled by microstructures in a periodical base cell (PBC). The homogenization method is used to derive the effective bulk modulus and thermal conductivity. BESO procedures are presented to optimize the two individual properties and their various combinations. Three numerical examples are studied. The results agree well with those of the benchmark microstructures and the Hashin-Shtrikman (HS) bounds.

Received: 20 October 2011; Accepted: 29 December 2011

KEYWORDS: Topology optimization; composite; homogenization; evolutionary structural method (ESO)

## 1. INTRODUCTION

Topology optimization has been an active research field for several decades. Among the various methods developed up to date, the material distribution model based on homogenization method has become widely popular since its original formulation by Bendsøe and Kikuchi [1]. One may refer to [2] for an extensive bibliography on the theory and

[*]Corresponding author: X.Y. Yang, School of Aerospace, Mechanical and Mechatronic Engineering, The University of Sydney, NSW 2006, Australia
[†]E-mail address: xiaoying.yang@rmit.edu.au

application of this method. Another class of method is based on Solid Isotropic Material with Penalization (SIMP) [3] which essentially applies a certain interpolation function and uses penalty to enforce an discrete (0,1) solution.

In both the homogenization and SIMP methods, the discrete problem is relaxed and a continuous design variable is used instead. Among a class of methods which directly deals with the discrete variable, evolutionary structural method (ESO) [4,5] has been developed extensively and has demonstrated its effectiveness. The original ESO uses the simple routine of gradually removing inefficient materials to reach an optimum. It is then formulated into a bidirectional ESO (BESO) where the materials are to be added if necessary [6]. More recently, BESO has been significantly improved in aspects such as the filter technique and material interpolations. This new version of BESO proves to be more robust and efficient [7,8]. It is also extended to address structures of two or multiple materials [9].

While topology optimization is originally developed for macrostructures, it is later formulated to tackle the microstructural or material design. In material design it is usually to find the optimal microstructures which fulfill the desired functions and properties. Central to its rapid development is the formulation of the inverse homogenization method which essentially applies topology optimization on a periodic base cell (PBC) [10-12]. Various material properties have been studied such as the bulk modulus [13], thermal expansion [14] and thermal conductivity [15-16]. The results are verified by good comparison to the analytical solutions [17-19], as well as the theoretical bounds such as the Hashin-Shtrikman (HS) bounds [20-21].

As the first attempt to address the microstructural or material design, the BESO method has been developed to optimize the bulk modulus and shear modulus for cellular materials [22]. In this paper it is to address the two-phase composite material with the properties of bulk modulus and thermal conductivity to be optimized. The two properties are optimized either independently or simultaneously.

The paper is organized as follows. It first briefly presents the calculation of the effective bulk modulus and thermal conductivity by the inverse homogenization, followed by the sensitivity analysis of the two properties. While the general equations for the sensitivity are well-known, a further derivation is conducted to facilitate the BESO implementation. The BESO procedure is then briefly presented. In the example section, the method is implemented on three examples. The results are discussed and compared with benchmarks. Then conclusions on the effectiveness of the method are made toward the end.

To keep the main text concise, details of sensitivity derivations are presented in the Appendix.

## 2. FORMULATION OF OPTIMIZATION PROBLEM

### *2.1 Effective properties and sensitivity analysis*

#### *2.1.1 Elastic properties*

The material consisting of different phases and/or viod is modeled by microstructures within a periodical base cell (PBC) which is discretized by *NE* finite elements. Using the homogenization theory [910-12], the homogenized or effective elastic tensor is expressed as

$$E_{ij}^{H} = \sum_{e=1}^{NE} Q_{ij}^{e} = \sum_{e=1}^{NE} \left( \frac{1}{Y^e} \int_{Y^e} (\boldsymbol{\varepsilon}_0^{i\,T} - \boldsymbol{\varepsilon}^{i\,T}) \mathbf{E} (\boldsymbol{\varepsilon}_0^{j} - \boldsymbol{\varepsilon}^{j}) dY_e \right)_e , \tag{1}$$

where $\mathbf{E}$ is the elastic constitutive matrix, $\boldsymbol{\varepsilon}_0$ is the unit test strain field and $\boldsymbol{\varepsilon}$ is the induced strain field. By denoting $Q_{ij}^{e} = \frac{1}{Y^e} \int_{Y^e} (\boldsymbol{\varepsilon}_0^{i\,T} - \boldsymbol{\varepsilon}^{i\,T}) \mathbf{E} (\boldsymbol{\varepsilon}_0^{j} - \boldsymbol{\varepsilon}^{j}) dY_e$ as the element mutual strain energy (where the superscript "*e*" means element), the effective elastic tensor is the summary of each element contribution.

For 2D microstructures, the bulk modulus is defined as $K = \sum_{i,j=1,2} c_{ij} E_{ij}^{H}$ with $c_{ij} = 1/4$. By substituting Eq. (1), $K$ can be expressed as

$$K = \sum_{i,j=1,2} c_{ij} \sum_{e=1}^{NE} Q_{ij}^{H} = \sum_{e=1}^{NE} \sum_{i,j=1,2} c_{ij} Q_{ij}^{H} = \sum_{e=1}^{NE} K^{e} \tag{2a}$$

$$\text{with } K^{e} = \sum_{i,j=1,2} c_{ij} Q_{ij}^{e} \tag{2b}$$

The sensitivity analysis can be conducted by using the adjoint method [1]. The equation for the sensitivity of $E_{ij}^{H}$ with respect to the design variable $x_e$ is given as

$$\frac{\partial E_{ij}^{H}}{\partial x_e} = \frac{1}{Y^e} \int_{Y^e} (\boldsymbol{\varepsilon}_0^{i\,T} - \boldsymbol{\varepsilon}^{i\,T}) \frac{\partial \mathbf{E}}{\partial x_e} (\boldsymbol{\varepsilon}_0^{j} - \boldsymbol{\varepsilon}^{j}) dY . \tag{3}$$

The term $\frac{\partial \mathbf{E}}{\partial x_e}$ is determined by the interpolation function assumed. Details of derivations of $\frac{\partial \mathbf{E}}{\partial x_e}$ and the subsequent $\frac{\partial K}{\partial x_e}$ are presented in the Appendix and the result as Eq. (A.7) is re-written here as

$$\frac{\partial K}{\partial x_e} = r_s^{m} K^{e} , \tag{4}$$

where $r_s^{m}$ is a constant for element of material *m*, as also detailed in the Appendix.

### *2.1.2 Thermal conductivity*

The governing equations for the elasticity and thermal conductivity are similar. Therefore, the effective thermal conductivity is similar to Eq. (1) and is expressed as

$$k_{ij}^H = \sum_{e=1}^{NE} R_{ij}^e = \sum_{e=1}^{NE} \left( \frac{1}{Y^e} \int_{Y^e} (\boldsymbol{\chi}_0^{i\,T} - \boldsymbol{\chi}^{i\,T}) \mathbf{k} (\boldsymbol{\chi}_0^j - \boldsymbol{\chi}^j) dY_e \right)_e , \tag{5}$$

where $\mathbf{k}$ is the material conductivity matrix, $\boldsymbol{\chi}_0$ is the unit temperature gradient field and $\boldsymbol{\chi}$ is the induced temperature gradient field. As $\mathbf{k}$ is a diagonal matrix, it follows that $k_{12}^H = k_{21}^H = 0$ for 2D microstructures.

The 'averaged' thermal conductivity is defined as the average of $k_{11}^H$ and $k_{22}^H$, i.e. , $s = \sum_{i=1,2} c_{ii} k_{ii}^H$ with $c_{ii} = 1/2$ . By substituting Eq. (5), $s$ is expressed as

$$s = \sum_{i=1,2} c_{ii} k_{ii}^H = \sum_{i=1,2} c_{ii} \sum_{e=1}^{NE} R_{ii}^e = \sum_{e=1}^{NE} \left( \sum_{i=1,2} c_{ii} R_{ii}^e \right) = \sum_{e=1}^{NE} s^e , \tag{6a}$$

$$\text{with } s^e = \sum_{i=1,2} c_{ii} R_{ii}^e \tag{6b}$$

The sensitivity of $k_{ij}^H$ with respect to the design variable $x_e$ is given as

$$\frac{\partial k_{ij}^H}{\partial x_e} = \sum_{e=1}^{NE} \left( \frac{1}{Y^e} \int_{Y^e} (\boldsymbol{\chi}_0^{i\,T} - \boldsymbol{\chi}^{i\,T}) \frac{\partial \mathbf{k}}{\partial x_e} (\boldsymbol{\chi}_0^j - \boldsymbol{\chi}^j) dY_e \right)_e , \tag{7}$$

Again from the Appendix, the sensitivity of the averaged thermal conductivity is found to be

$$\frac{\partial s}{\partial x_e} = r_c^m s^e , \tag{8}$$

where $r_c^m$ is a constant for element of material *m*.

*2.2 Objective function and optimization implementation*

The optimization objective function is defined as

$$\text{Minimize } f = h_s \frac{(K - K_u^*)^2}{K_u^{*2}} + h_c \frac{(s - s_u^*)^2}{s_u^{*2}} , \tag{9a}$$

$$\text{Subjected to } V_e x_e = V , \; x_e = x_{\min} \text{ or } 1 \tag{9b}$$

where $K_u^*$ and $s_u^*$ are the upper bounds, $x_e$ is the design variable with $x_e$ =0 (or $x_e = x_{\min}$) as material 1 and $x_e$ =1 as material 2. $V$ is the volume fraction for material 2. $h_s$ and $h_c$ are

the weighing factors with $h_s + h_c = 1$ . With $h_c = 0$, the objective function is reduced to a single bulk modulus case and with $h_c = 1$ it is a single thermal conductivity case.

From the Appendix, the sensitivity of the above objective function is given as

$$\frac{\partial f}{\partial x_e} = 2h_s d_s c_s^m K^e + 2h_c d_c c_c^m s^e, \tag{10}$$

where the factors of $d_s$, $c_s^m$, $d_c^e$ and $c_c^m$ are detailed in the appendix too.

The BESO algorithms remain largely the same as that for the macrostructural optimization. Only minor additions are made such as at each iteration updating the unit strain/temperature gradient. As the algorithms and its parameters have been introduced and explained at length in most BESO literature, they are presented here only briefly. One may refer to the most recent literature [2121] for more detailed presentations.

The major parameters involved in BESO algorithms are the filter radius $r_{\min}$, the evolution ratio (*ER*) and additional ratio (*AR*) and the convergence $t$ tolerance. The filter radius specifies the range within which the element sensitivity is to be smoothened. The two parameters of *AR* and *ER* dictate at each iteration the number of elements to be modified. The iteration will terminate once the target volume constraint has been reached and the objective function has flattened (i.e. relative difference between iterations $< t$ ).

The BESO procedures are as follows.

1. Discretize the periodic base cell with finite elements and apply boundary conditions.
2. Apply unit strain fields/temperature gradient fields. Conduct FEM analysis to obtain the solution, i.e., $\boldsymbol{\varepsilon}$ and $\boldsymbol{\chi}$.
3. Calculate the effective properties using Eqs. (1) and (5) and the objective function using (9).
4. Calculate the sensitivity for each element using Eqs. (4), (8), or (10). Apply the filter technique based on the radius of $r_{\min}$.
5. "Downgrade" elements of the smallest sensitivity, and "upgrade" element of the largest sensitivity.
6. Update element status, and repeat steps 2 to 5 until the solution is converged.

## 3. EXAMPLES

*Example 1: maximizing the bulk modulus*

In this example it is to maximize the bulk modulus for the microstructure consisting of two base materials. The elastic properties are as per the example in reference [1213], that is, the Young's modulus is $E_1 = 0.05$, $E_2 = 1.0$ with a common Poisson's ratio of 0.3. Their corresponding bulk modulus and shear modulus are $K_2 = 5/7$, $K_1 = K_2/20$, $G_2 = 5/13$ and $G_2 = G_1/20$. The volume constraint is set as $V = 50\%$, and the upper HS bound of the

effective bulk modulus is $K_u^*$=0.2235. There are known optimal microstructures such as the single-length-scale Vigdergauz type microstructures [1718,19] and the two-length-scale polycrystal microstructures [1213].

To find the optimal results using BESO, three initial domains are considered, as shown in Figure 1. The square design domain in Figure 1(a) is a mesh of 80×80 and the rectangular domain in Figure 1(b)&(c) is a mesh of 104×60. The green (dark) elements represent the base material 2 (which is 'stronger' with $K_2 > K_1$ ), and the pink (light) elements in the centre represent material 1. Elements of material 1 are a circular sub-domain within the ground structure. In this case the diameter of the circle is D=0.1 of the larger side length of the design domain.

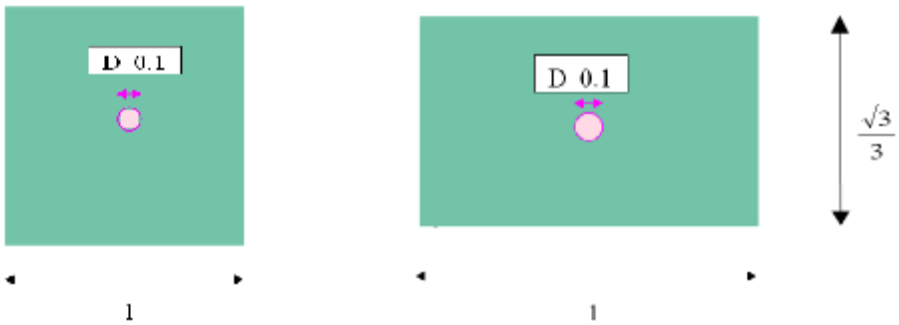


(a) square symmetrical square initial structure

(b) 90 degree symmetrical rectangular domain, with aspect ratio of $\sqrt{3}/3$

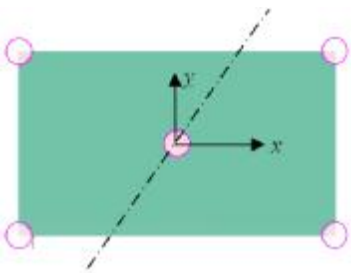


(c) 60 degree symmetrical rectangular domain, with aspect ratio of $\sqrt{3}/3$

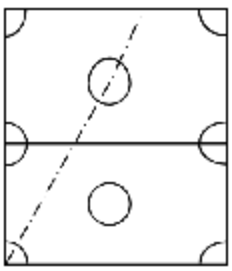

(c) Axis of symmetry for the rectangular domain in Figure (c)

Figure 1. Initial design domain

The rectangular domain in Figure 1(b) and (c) has an aspect ratio of $\frac{\sqrt{3}}{3}$. In Figure 1(b) the domain consists of one region of material 1 which is in the centre. In Figure 1(c), the domain has four additional quarter circles at each corner and the diameter is the same as the circle in the centre. As illustrated in Figure 1(d), this initial design is hexagonally symmetrical, which is to promote isotropy of the resulting design [23, 24].

The interpolation function for the Young's modulus is taken as Eq. (A.1) with $p$=2 and $x_{\min}$ =1.0e-3. The BESO parameters are $ER$=1%, $AR$=20%, $r_{\min}$ =8 elements and $t$ =1%. The microstructures of maximum bulk modulus are presented in Figure 2. The hexagonal

microstructures in Figure 2(c) agree well with that obtained by Sigmund [13]. The values of the bulk modulus for these topologies are very close, i.e. $K$ =0.2213, 0.2217 and 0.2208 respectively, which are all above 98% of the HS bound. The number of iterations taken to reach the optimum is less than 90 in all the cases.

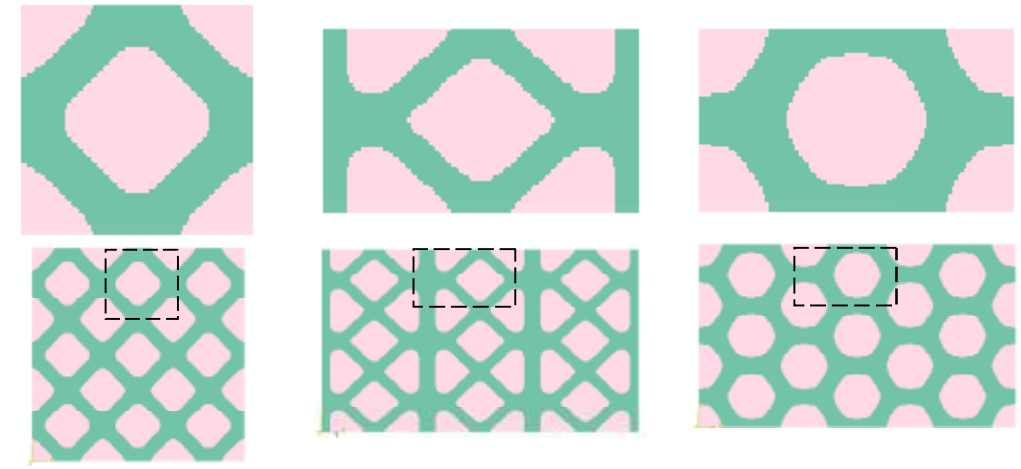

$$\begin{bmatrix} 0.2808 & 0.1635 & 0.0000 \\ 0.1635 & 0.2808 & 0.0000 \\ 0.0000 & 0.0000 & 0.15318 \end{bmatrix} \qquad \begin{bmatrix} 0.2999 & 0.1297 & 0.0000 \\ 0.1297 & 0.3241 & 0.0000 \\ 0.0000 & 0.0000 & 0.1170 \end{bmatrix} \qquad \begin{bmatrix} 0.3218 & 0.1234 & 0.0000 \\ 0.1234 & 0.3166 & 0.0000 \\ 0.0000 & 0.0000 & 0.0991 \end{bmatrix}$$

$K$=0.2222 Microstructures from initial design(a)

$K$=0.2208 Microstructures from initial (b)

$K$=0.2213 Microstructures from initial (c)

Figure 2. Optimal microstructures of maximum bulk modulus
Rows are for 1×1 base cell, 3×3 base cell, effective elastic matrix and bulk modulus

It is seen that the volume constraint $V$ =50% is approached gradually as the iteration starts with a high volume, in this case $V$ =90%. It is possible to start with an initial design which is close to the constraint volume. The volume constraints can be approximated by modifying the size of the circle in the initial design domain as shown in Figure 1(a). Again take $V$ =50% for example, by increasing the diameter from 0.1 to 0.8 the volume of material 2 becomes $V$ =49.6% as shown in Figure 3(a). The resulting topology displays an octagonal microstructure which is again similar to Sigmund's results [13]. The effective elastic matrix is also shown in Figure 3(a) and its corresponding bulk modulus is $K$=0.2216 which is very close to the values presented in Figure 2.

The advantage of using an initial design of approximate volume is that the number iterations taken can be significantly reduced. This is demonstrated in Figure 4 where two initial designs are compared. Starting with a high volume, the bulk modulus decreases as a result of volume reduction. After the volume approaches the constraint, the change is flattened which indicates that the microstructure is more or less fine-tuning itself until it reaches an optimum. This kind of fine change is seen from the start when the initial design already approximates the volume constraint. The number of iterations now is close to 20, as compared

to 90.

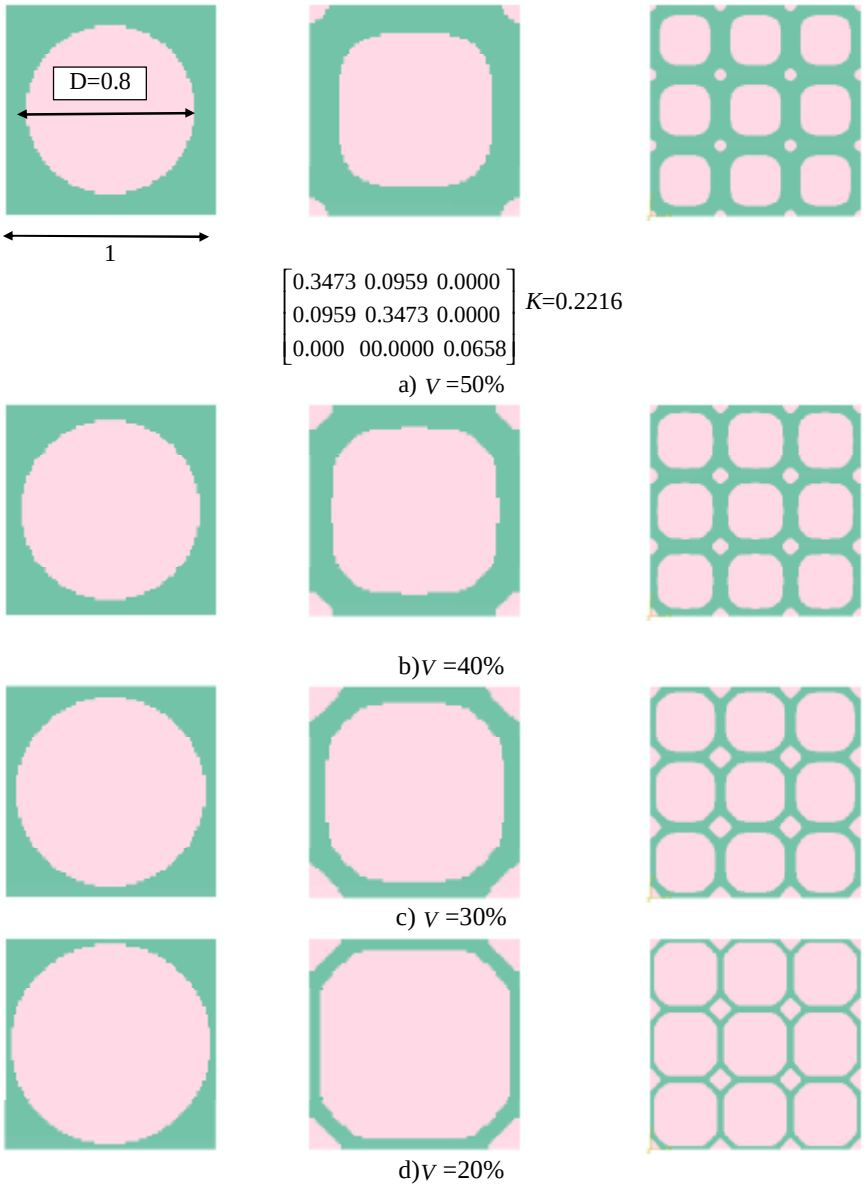


Figure 3. Octagonal microstructures of maximum bulk modulus. Columns are for initial design, optimal microstructure of 1×1 base cell and 3×3 base cell

Compare all the topologies in Figures 2&3, it is seen that the final topology varies with the initial design. The effect of initial design is discussed in many literatures e.g. Refs. [15, 23] and it is well recognized that the solution to the topology optimization is highly non-unique.

Three more cases of different volume constraints have been studied and the results are shown Figure 3. It is seen that the microstructures take the shape of an octagon and the cell wall becomes thinner as the volume is reduced.

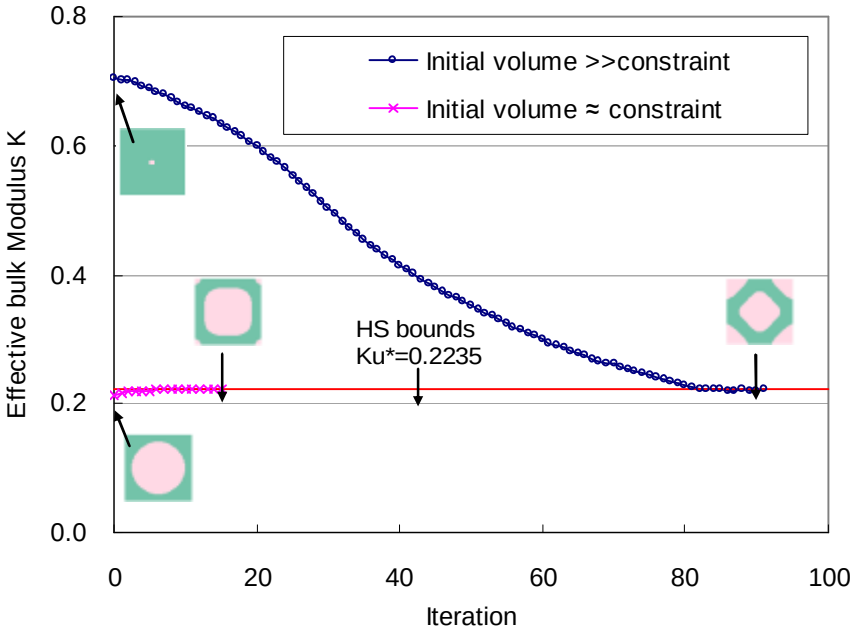


Figure 4. Iteration histories for a) initial volume of material 2 >> volume constraint, and b) full Initial volume of material 2≈volume constraint

Similarly, for the initial rectangular design domain as shown in Figure 1(c), the diameter of the five circles/quarter-circles can be modified so that the volume is close to the constraint. Initial designs for the above four volume constraints are shown in Figure 5. While they may appear more complex than a usual central-holed square, they are generated easily just by adding several lines in the related subroutine. It is seen that those initial designs are very similar to their 'intended' hexagonal honeycomb optimum. So it is not surprising that the convergence is fast. The number of iterations in all four cases is less than 15.

In Figure 6, the above octagonal and hexagonal microstructures are compared to the HS bound. The values of effective bulk modulus in all cases are above 98% of the bound. The elastic matrix of the hexagonal microstructure with $V$ =50% is shown in Figure 5(a) and its bulk modulus is very close to that of the octagonal microstructures.

*Example 2: Optimizing the bulk modulus and thermal conductivity*

The properties of the two base materials are as per the example of reference [15], that is, the Young's modulus is $E_1$ =1.0 and $E_2$ =3.0 with a common Poisson's ratio of 0.3, and the thermal conductivity is $s_1$ =3.0 and $s_2$ =1.0. The composite is non well ordered as each constituent is larger in one property but smaller in the other, i.e. $(E_1 - E_2)(s_1 - s_2)<0$. This means that in optimization the two properties cannot approach their respective bound (e.g. HS bound) simultaneously.

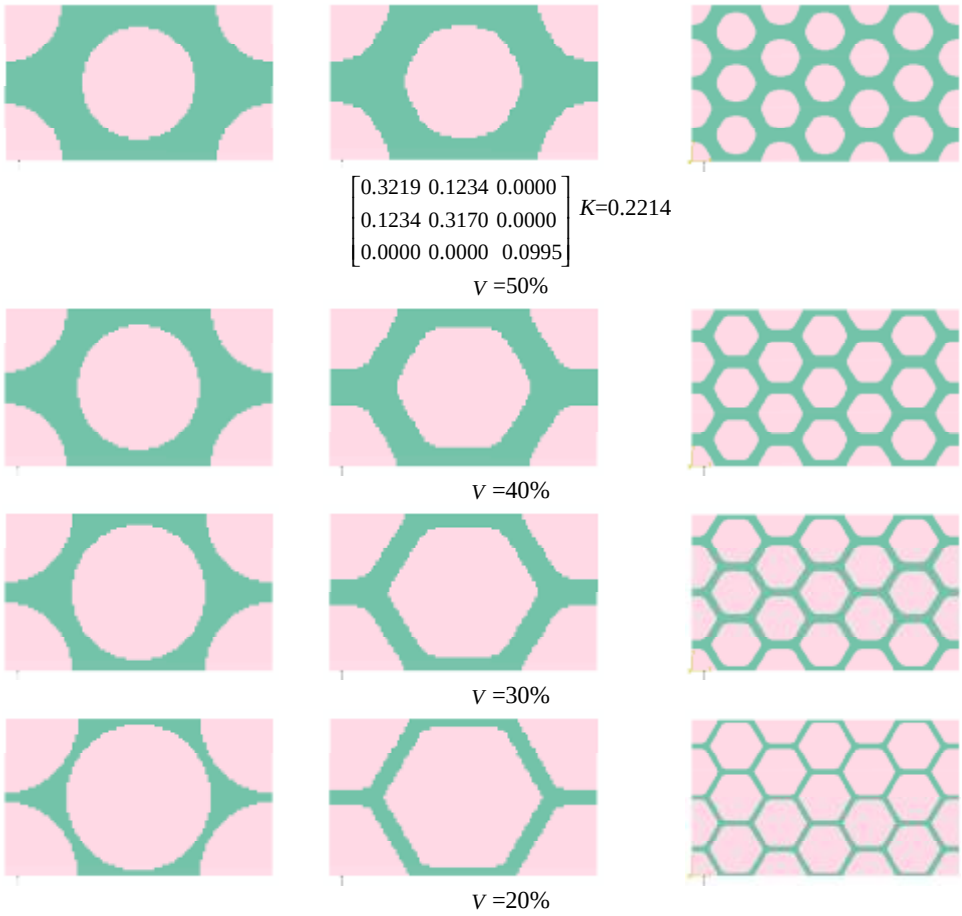


Figure 5. Hexagonal microstructures of maximum bulk modulus
Columns are for initial design, optimal microstructure of 1×1 base cell and 3×3 base cell

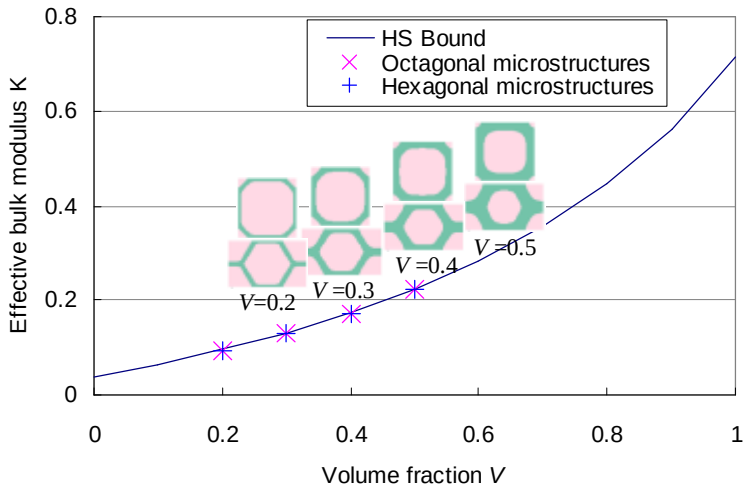


Figure 6. Effective bulk modulus for a) octagonal microstructures, and b) hexagonal microstructures

The volume constraint in this example is set as $V$ =50%. The interpolation function for the Young's modulus is taken as Eq. (A.3) with $q$=1.5. The interpolation function for the thermal conductivity is based on the lower HS bound in Eq. (A.9b). The BESO parameters are $ER$=1%, $AR$=20%, $r_{\min}$ =2 elements and $t$ =0.5%.

As shown in Figure 7, the square design domain is divided by an 80×80 mesh and two initial designs are defined. The initial design 1 (in the first row) has material 2 as the outer layer and material 1 as the inclusion, and in design 2 (in the second row) the two materials are swapped. It is evident that design 1 has a higher bulk modulus and design 2 has a higher thermal conductivity.

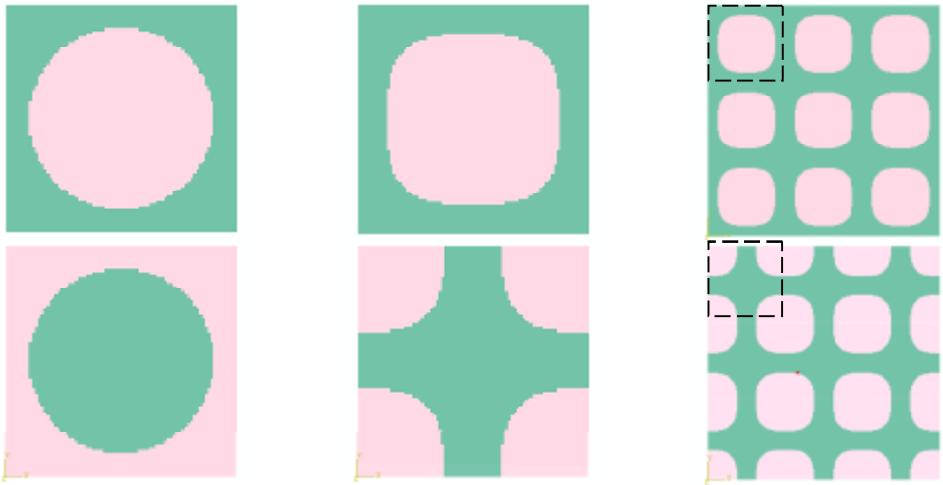

Elastic matrix:

$$\begin{bmatrix} 1.9331 & 0.5283 & 0.0000 \\ 0.5283 & 1.9331 & 0.0000 \\ 0.0000 & 0.0000 & 0.6018 \end{bmatrix}$$

Bulk modulus $K$=1.2307

Thermal conductivity $\sigma$ =1.6689

Figure 7. Microstructures for maximized bulk modulus ($h_c$ =0)
Columns are for initial design, optimal microstructure of 1×1 base cell and 3×3 base cell

First we consider two single cases of maximizing the bulk modulus (Figure 7), and thermal conductivity (Figure 8) separately, i.e. $h_c$ =0 and $h_c$ =1. It is shown in Figure 7. that the microstructures from the two initial designs are identical. Similarly, the two microstructures as shown in Figure 8 are identical too. Also compare $h_c$ =0 with $h_c$ =1, it is noted that their corresponding microstructures are inversion of each other.

The elastic matrixes, bulk modulus and thermal conductivity agree well with those previously reported [15]. The maximum bulk modulus obtained is 97.9% of the HS bound, and the maximum thermal conductivity is 99.9% of the HS bound. The number of iterations are less than 40 in all these cases, comparing to 25 (bulk modulus) and 80 (conductivity) in the same literature.

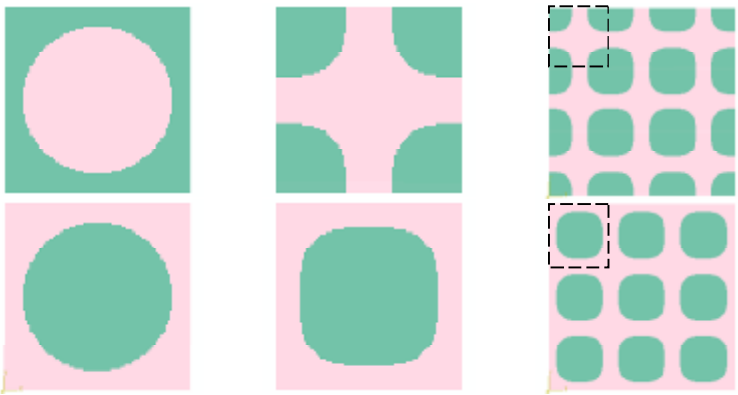


Figure 8. Microstructures for maximized thermal conductivity ($h_c$=1)
Columns are for initial design, optimal microstructure of 1×1 base cell and 3×3 base cell

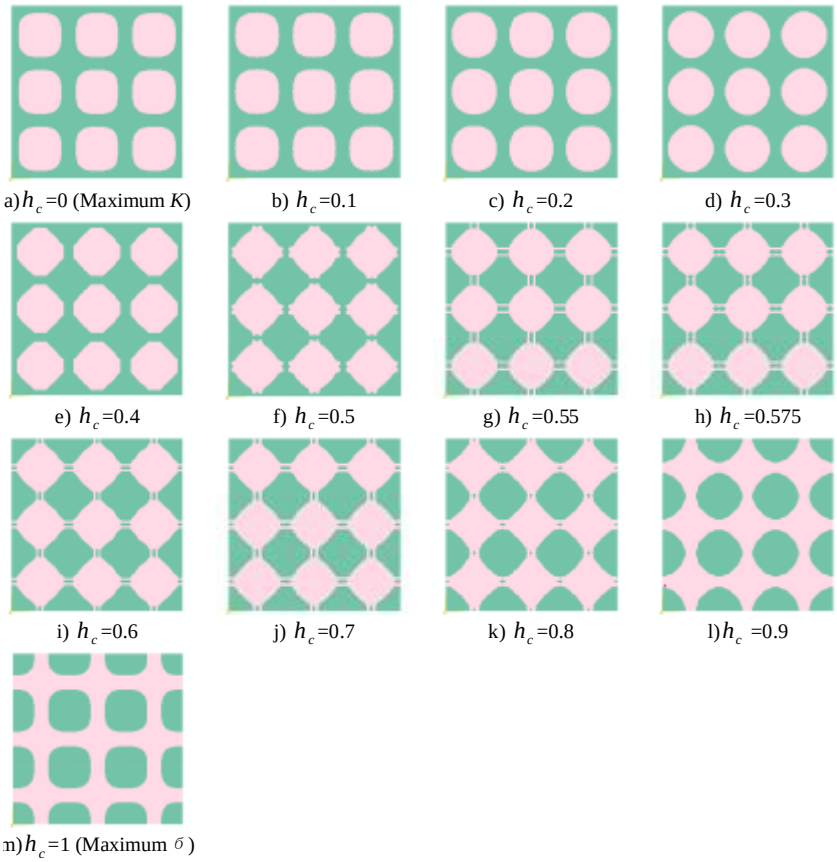


Figure 9. Microstructures for optimum of combined bulk modulus and thermal conductivity, based on initial design 1

Figure 9 presents microstructures of $h_c$ varying from 0 to 1 based on initial design 1. It is shown that the boundary of the two phases changes gradually to transform from a near square inclusion to an open cross channel. The change is very small between $h_c$=0 to 0.2 and this is reflected by their corresponding points in Figure 11 which are closely spaced to each other. At $h_c$= 0.3 the initial inclusion transitions to a near circular shape, then material 2 (the conductive phase) further infiltrates to the insulating phase orthogonally. At $h_c$=0.55 the infiltration leads to the cell edge and as a result thin conductive channels are formed. The channels then grow larger and the conductivity is further increased until it reaches the maximum at $h_c$=1.

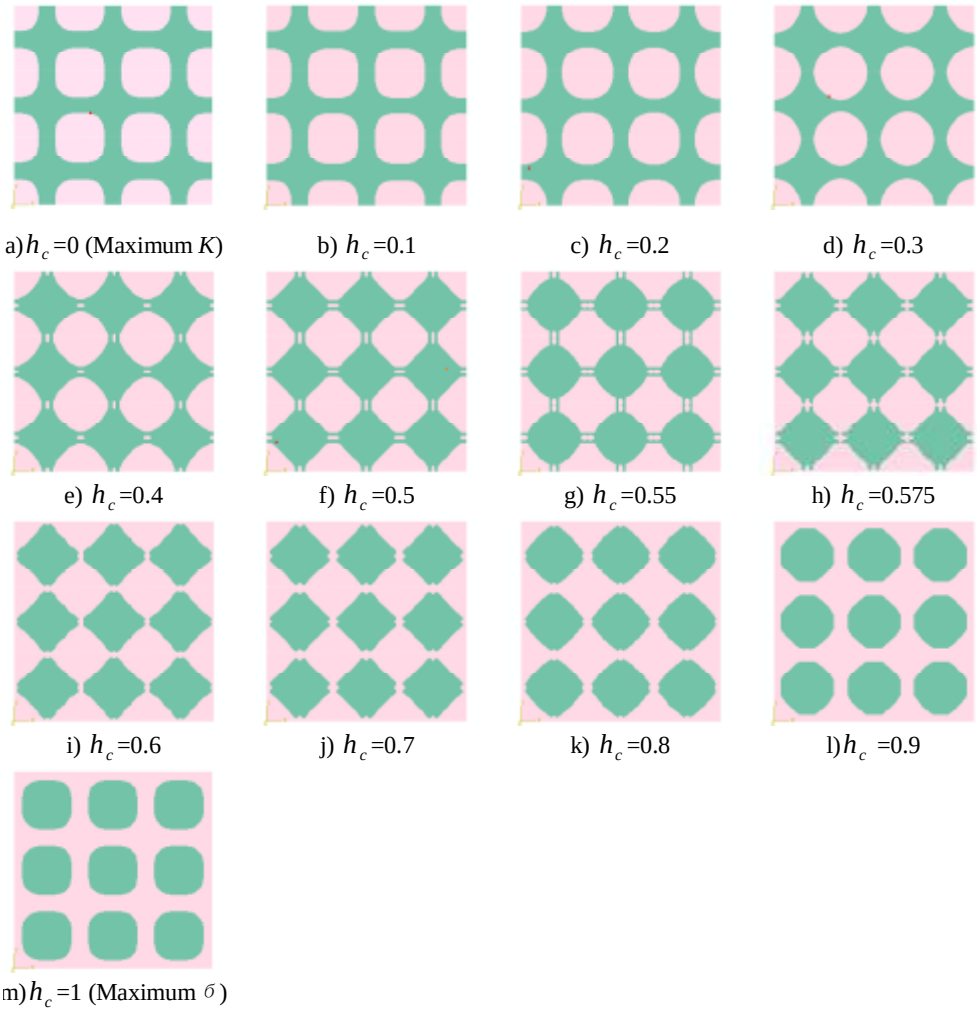


Figure 10. Microstructures for combined bulk modulus and thermal conductivity, based on initial design 2

Figure 10 presents microstructures of $h_c$ varying from 0 to 1 based on initial design 2.

While the topologies obtained from the above two initial designs are different, the values of bulk modulus and thermal conductivity are very close and the difference is less than 0.3%.

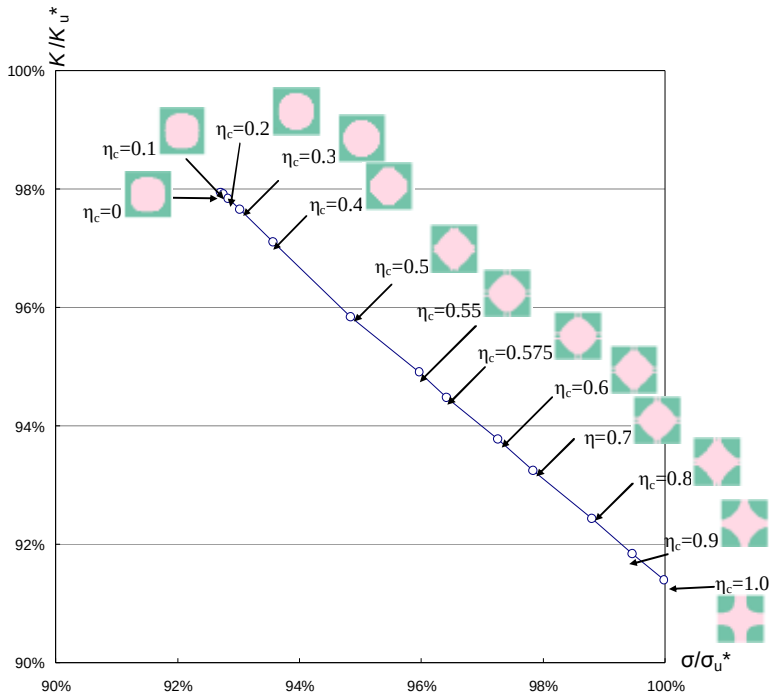


Figure 11. Bulk modulus vs. effective thermal conductivity for a range of $h_c$ from 0 to1

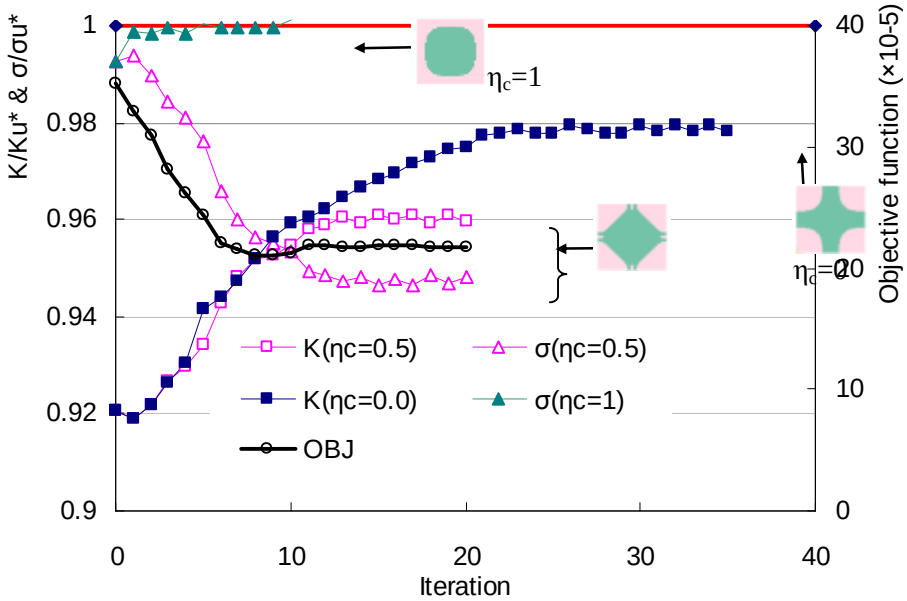


Figure 12. Iteration histories for a) maximum bulk modulus $h_c$=0, b) maximum conductivity $h_c$=1.0, and c) combined bulk modulus and conductivity $h_c$=0.5

In Figure 11, the bulk modulus and thermal conductivity based on initial design 1 are plotted. It displays compromise between these two properties as $h_c$ varying from 0 to 1. In Figure 12, the iteration history is presented for three cases, i.e. $h_c$=0, $h_c$=0.5 and $h_c$=1 based on initial design 2. It is seen that for $h_c$=0 and $h_c$=1, the bulk modulus and thermal conductivity increase throughout the iteration and reach their individual maximum. For the combined case, the conductivity is reduced while the bulk modulus is increased. As the initial structure is conductivity dominant, the number of iteration is the smallest for $h_c$=1, followed by $h_c$=0.5 and then $h_c$=0.

*Example 3: Minimizing thermal conductivity*

The same phase materials as in example 2 are used and the thermal conductivity is to be minimized. The objective function takes the same form as Eqs. (9a)&(9b) with $h_c$=1 and $s_u^*$ being replaced with $s_l^*$ which is the lower HS bound. To implement the sensitivity analysis Eq. (A.9a) for the HS upper bound is used as the interpolation function.

Starting from the initial design 2, the initial conductivity is high as the insulating phase (dark) is enclosed. Through some 30 iterations the insulating phase is extended to the cell edge which finally forms an enclosure to the conductive phase, as shown in Figure 13. It coincides with the topology with the maximum bulk modulus as shown in Figure 10(a). Its thermal conductivity is 1.669 compared to the lower bound $s_l^*$=1.667.

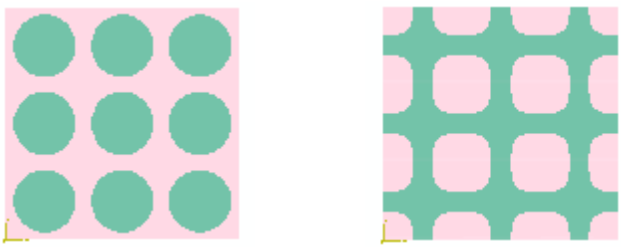

a) Initial design b) Final design

Figure 13. Microstructures for minimizing thermal conductivity, based on initial design 2

## 4. CONCLUSION

The BESO method is extended to the design of two phase composite materials with single or multiple objective functions considered. For optimization of single bulk modulus and single thermal conductivity, the results agree well with the benchmark microstructures which attain the HS bounds. For the two-objective optimization, the results display gradual transition of intermediate designs from one objective to the other. While the design topologies vary with the initial design in most cases, the values of the modulus/conductivity and the objective function are very close. The number of iterations is around 90 or around 40 depending on the initial

design. It is demonstrated that the BESO method is effective and efficient in optimizing the bulk modulus, thermal conductivity, and their combinations.

**Acknowlegement:** The work conducted in this paper is supported by Australian Research Council under its Discovery Projects funding scheme (Project No. DP1094403). The authors are grateful to Dr. S.W. Zhou of The University of Sydney for valuable advice.

## REFERENCES

1. Bendsøe MP, Kikuchi N. Generating optimal topologies in structural design using a homogenization method, *Comput Methods Appl Mech Eng* 1988; **71:**197-224.
2. Bendsøe MP, Sigmund O, *Topology Optimization - Theory, Methods and Applications*, 2nd ed., Springer, Berlin, 2003.
3. Rozvany GIN, Zhou M, Birker T. Generalized shape optimization without homogenization. *Struct Optim* 1992; **4:** 250-54.
4. Xie YM, Steven GP. A simple evolutionary procedure for structural optimization. *Comput Struct* 1993; **49:** 885-96.
5. Xie YM, Steven GP. *Evolutionary Structural Optimization*, Springer-Verlag, London, 1997.
6. Yang XY, Xie YM, Steven GP, Querin OM. Bi-directional evolutionary method for stiffness optimization. *AIAA J* 1999; **37**:1483-88.
7. Huang X, Xie YM. *Evolutionary Topology Optimization of Continuum Structures: Methods and Applications*, John Wiley & Sons, Chichester, 2010.
8. Huang X, Xie YM, Burry MC. Convergent and mesh-independent solutions for the bi-directional evolutionary structural optimization method, *Finite Elem Anal Des* 2007; **14:** 1039-49.
9. Huang X, Xie YM. Bi-directional evolutionary topology optimization of continuum structures with one or multiple materials, *Comp Mech* 2009; **3:**393-401.
10. Sigmund O. Tailing materials with prescribed elastic properties, *Mech Mater* 1994; **20**:351-68.
11. Hassani B, Hinton E. A review of homogenization and topology opimization I - hompgenization thory for media with periodic structure, *Comput Struct* 1998;**69:**707-17.
12. Hassani B, Hinton E. A review of homogenization and topology optimization II - analytical and numerical solution of homogenization Eq.s, *Comput Struct* 1998;**69**:719-38.
13. Sigmund O. A New Class of Extremal Composites, *J Mech Phys Solids* 2000;**48**:397-528.
14. Sigmund O, Torquato S, Design of materials with extreme thermal expansion using a three-phase topology optimization method, *J Mech Phys Solids* 1997; **6**:1037–67.
15. Kruijf ND, Zhou SW, Li Q, Mai YW. Topological design of structures and composite materials with multiobjectives, *Int J Solids Struct* 2007; **44**:7092-109
16. Zhou SW, Li Q. Computational design of multi-phase microstructural materials for

extremal conductivity, *Comp Mater Sci* 2008; **43**:549-64.
17. Gibson LJ, Ashby MF. *Cellular Solids: Structure and Properties,* 2nd ed., Cambridge University Press, 1998.
18. Vigdergauz SB. Regular structures with extremal elastic properties, *Mech Solids* 1989; **24**:57–63.
19. Vigdergauz SB. Energy-minimizing inclusion in a planar elastic structure with macroisotrophy, *Struct Optim* 1999; **17**:104-12.
20. Hashin Z, Shtrikman S. A variational approach to the theory of the effective magnetic permeability of multiphase materials. *J Appl Phys* 1962; **35**:3125-31.
21. Hashin Z, Shtrikman S. A Variational Approach to the Theory of the Elastic Behaviour of Multi-phase Materials, *J Mech Phys Solids* 1963; **11**:127-40.
22. Huang X, Radman A, Xie YM. Topological design of microstructures of cellular materials for maximum bulk or shear modulus, *Comp Mater Sci* 2011; **50:**1861-70.
23. Guedes JM, Rodrigues HC, Bendsøe MP. A material optimization model to approximate energy bounds for cellular materials under multiload conditions, *Struct Optim* 2003; **25**:446–52.
24. Hyun S, Torquato S. Optimal and manufacturable two-dimensional, Kagomé-like cellular solids, *J Mater Res* 2002; **17**:137-44.
25. Stolpe M, Svanberg K. An alternative interpolation scheme for minimum compliance topology optimization, *Struct Optim* 2001; **22**:116–24.

## APPENDIX

In the following presentation, it is assumed that the two base materials have $E_2 > E_1$ and $k_2 < k_1$, and a common Poisson's ratio *v*.

### A1. Sensitivity of bulk modulus

Case 1: Based on SIMP[2,8], the interpolation for Young's modulus is given as

$$E(x_e) = E_2 x_e^p + E_1(1 - x_e^p), \tag{A.1}$$

where *p* is the penalty factor. Its derivative with respect to the design variable $x_e$ is

$$\frac{\partial E}{\partial x_e} = p x_e^{p-1}(E_2 - E_1) \tag{A.2}$$

Case 2: The interpolation based on the Eq. proposed by Stolpe and Svanberg [24] is given as

$$E(x_e) = E_1 + \frac{x_e(E_2 - E_1)}{1 + q(1 - x_e)} \tag{A.3}$$

The factor is $q$ is similar to the penalty used in SIMP. Its derivative is expressed as

$$\frac{\partial E}{\partial x_e} = \frac{x_e q(E_2 - E_1)}{(1+q(1-x_e))^2} + \frac{(E_2 - E_1)}{1+q(1-x_e)} \tag{A.4}$$

At $x_e$=0 and $x_e$=1, $\frac{\partial E}{\partial x_e}$, it can be written as function of $E_1$ and $E_2$. Denoting $E_m$ to representing $E_1$ or $E_2$ where the subscript "$m$" means the material, it follows that

$$E = E_m \tag{A.5 a}$$

$$\frac{\partial E}{\partial x_e} = r_s^m E_m \tag{A.5b}$$

$$\frac{\partial \mathbf{E}}{\partial x_e} = r_s^m \mathbf{E}_m \tag{A.5c}$$

where $r_s^m$ is calculated from Eq. (A.2) by substituting $x_e$=0 or $x_e$=1 (the superscript "s" means stiffness) . As it is assumed that the two base material has a common Poisson's ratio, i.e. $\frac{\partial \nu}{\partial x_e}$=0, $\frac{\partial \mathbf{E}}{\partial x_e}$ is function of $\frac{\partial E}{\partial x_e}$ only and therefore the coefficient $r_s^m$ is the same in Eqs. (A.5b) & (A.5c).

The sensitivity of the effective elastic tensor is given as

$$\frac{\partial E_{ij}^H}{\partial x_e} = \frac{1}{Y^e}\int_{Y^e}(\boldsymbol{\varepsilon}_0^{i\,T} - \boldsymbol{\varepsilon}^{i\,T})\frac{\partial \mathbf{E}}{\partial x_e}(\boldsymbol{\varepsilon}_0^j - \boldsymbol{\varepsilon}^j)dY = r_s^m \frac{1}{Y^e}\int_{Y^e}(\boldsymbol{\varepsilon}_0^{i\,T} - \boldsymbol{\varepsilon}^{i\,T})\mathbf{E}(\boldsymbol{\varepsilon}_0^j - \boldsymbol{\varepsilon}^j)dY = r_s^m Q_{ij}^e \tag{A.6}$$

Combining the above equation. and that $K^e = \sum_{i,j=1,2} c_{ij} Q_{ij}^e$, it is found

$$\frac{\partial K}{\partial x_e} = r_s^m K^e \tag{A.7}$$

As $K^e$ is the contribution of the $e$th element to the bulk module $K$, it is meant in Eq. (A.5) that the sensitivity of this element is the its contribution scaled by a factor $r_s^m$, that is $r_s^1$ for all elements of material 1 and $r_s^2$ for elements of material 2.

**A2. Sensitivity of thermal conductivity**

The constitutive matrix for the two base materials is given as

$$\mathbf{k}_m = \begin{bmatrix} k_m & 0 \\ 0 & k_m \end{bmatrix}, \tag{A.8}$$

where the subscript "*m*" denotes material 1 or 2.

The Hashin-Shtrikman bounds [20] are as below

$$\begin{cases} \text{Upper bound } s_u^* = -k_1 + \dfrac{1}{\dfrac{x_e}{k_2 + k_1} + \dfrac{1 - x_e}{k_1 + k_1}} & \text{(A.9a)} \\ \text{Lower bound } s_l^* = -k_2 + \dfrac{1}{\dfrac{1 - x_e}{k_1 + k_2} + \dfrac{x_e}{k_2 + k_2}} & \text{(A.9b)} \end{cases}$$

For the objective of maximizing the thermal conductivity, the lower bound is taken as the interpolation function, and vice versa. The following derivation takes the lower bound as example and it is equally applicable to the high bound. The simple way is to interchange $k_1$ and $k_2$, and $x_e$ and $1 - x_e$.

The derivative of the lower bound interpolation is as below

$$\frac{\partial k}{\partial x_e} = \frac{\partial s_l^*}{\partial x_e} = -\frac{(b-a)}{\left((b-a)x_e + a\right)^2}, \tag{A.10a}$$

$$\text{where } a = \frac{1}{k_1 + k_2} \text{ and } b = \frac{1}{k_2 + k_2}$$

Similar to the derivation for the bulk modulus case, at $x_e$ =0 and $x_e$ =1, it follows that

$$\begin{cases} k = k_m & \text{(A.11a)} \\ \dfrac{\partial k}{\partial x_e} = r_c^m k_m & \text{(A.11b)} \\ \dfrac{\partial \mathbf{k}}{\partial x_e} = r_c^m \mathbf{k}_m & \text{(A.11c)} \\ \dfrac{\partial s}{\partial x_e} = \dfrac{\partial s^e}{\partial x_e} = r_c^m s^e & \text{(A.11d)} \end{cases}$$

$r_c^m$ (i.e. $r_c^1$ and $r_c^2$) is calculated from Eq. (A.10a) by substituting $x_e$ =0 or $x_e$ =1. It is shown that the element sensitivity $\dfrac{\partial s}{\partial x_e}$ is equal to the element contribution $s^e$ to the thermal

conductivity scaled by the factor $r_c^m$.

**A3. Nomination of sensitivity for two-objective optimization**

The sensitivity of Eq. (9a) in the Section 2.2 is expressed as

$$\frac{\partial f}{\partial x_e} = 2h_s \frac{(K - K_u^*)}{K_u^*} \frac{\frac{\partial K}{\partial x_e}}{K_u^*} + 2h_c \frac{(s - s_u^*)}{s_u^*} \frac{\frac{\partial s}{\partial x_e}}{s_u^*} \tag{A.12}$$

Substituting Eqs. (A.7) & (A.11d) to the above we obtain

$$\frac{\frac{\partial K}{\partial x_e}}{K_u^*} = r_s^m \frac{K^e}{K_u^*} \tag{A.13a}$$

$$\frac{\frac{\partial s}{\partial x_e}}{s_u^*} = r_c^m \frac{s^e}{s_u^*} \tag{A.13b}$$

The two terms $\frac{K^e}{K_u^*}$ and $\frac{s^e}{s_u^*}$ are dimensionless and they are both less than 1 (it can be understood as the percentage of element contribution comparing to the bound). It is necessary for the Eqs. (A.13a) & (A.13b) to be in a similar order regardless of the interpolation functions used. This is explained through example 2 of the Section 3 where the properties are given as $E_1$ =1.0 and $E_2$ =3.0, $k_1$ =3.0 and $k_2$ =1.0. The derived factors are listed in Table 1.

Table 1: Factors to calculate the sensitivity for bulk modulus and thermal conductivity

| **Item** | **Material 1($x_e$ =0)** | **Material 2($x_e$ =1)** |
|---|---|---|
| Bulk modulus, 1) $q$=1.5 | $r_s^1$ =4/5 | $r_s^2$ =5/3 |
| Bulk modulus, 2) $q$=3 | $r_s^1$ =1/2 | $r_s^2$ =8/3 |
| Thermal conductivity | $r_c^1$ =-4/3 | $r_c^2$ =-1 |

In Table 1, it is shown that for the bulk modulus case, the factors $r_s^1$ and $r_s^2$ are changed with $q$ changing from 1.5 to 3. For the conductivity case, we choose that its interpolation remains unchanged (that is, $r_c^1$ and $r_c^2$ stay the same). Therefore the change of $q$ is similar to artificially altering the proportion for the bulk modulus case. This is to be avoided and it is necessary to normalize factors of $r_s^1$, $r_s^2$, $r_c^1$ and $r_c^2$. The method used here is as follows.

1. For the bulk modulus case, find the absolute maximum of the "original" sensitivity, i.e., $\frac{\frac{\partial K}{\partial x_e}}{K_u^*} = r_s^m \frac{K_m^e}{K_u^*}$ for both material 1 and material 2. They are written as $M_1^s = max\left| r_s^1 \frac{K_1^e}{K_u^*} \right|$ and $M_2^s = max\left| r_s^2 \frac{K_2^e}{K_u^*} \right|$ respectively. Average the maximum of the two materials by $M^s = \frac{1}{2}(M_1^s + M_2^s)$.

2. Likewise, for the thermal conductivity case, find $M_1^c = max\left| r_c^1 \frac{s_1^e}{s_u^*} \right|$ and $M_2^c = max\left| r_c^2 \frac{s_2^e}{s_u^*} \right|$ and their average $M^c = \frac{1}{2}(M_1^c + M_2^c)$.

3. Normalize $\frac{\frac{\partial K}{\partial x_e}}{K_u^*}$ by $M^s$, and $\frac{\frac{\partial s}{\partial x_e}}{s_u^*}$ by $M^c$,i.e.

$$\frac{\frac{\partial K}{\partial x_e}}{K_u^*} \Big/ M^s = \frac{r_s^m}{M^s} \frac{K^e}{K_u^*} = c_s^m \frac{K^e}{K_u^*} \tag{A.1a}$$

$$\frac{\frac{\partial s}{\partial x_e}}{s_u^*} \Big/ M^c = \frac{r_c^m}{M^c} \frac{s^e}{s_u^*} = c_c^m \frac{s^e}{s_u^*}, \tag{A.14b}$$

where $c_s^m = \frac{r_s^m}{M^s}$ and $c_c^m = \frac{r_c^m}{M^c}$.

The above normalization is incorporated to Eq. (A.12). Denoting $d_s = \frac{(K - K_u^*)}{K_u^*}$ and $d_c = \frac{(s - s_u^*)}{s_u^*}$, the final sensitivity is given as

$$\frac{\partial f}{\partial x_e} = 2h_s d_s c_s^m K^e + 2h_c d_c c_c^m s^e \tag{A.15}$$